Biophysical Chemistry 145 (2009) 116–125

Contents lists available at ScienceDirect

Biophysical Chemistry

journal homepage: http://www.elsevier.com/locate/biophyschem

New insights into DNA-binding behavior of Wilms Tumor Protein (WT1) — A dual study

Elmar Nurmemmedov [a,1], Raymond K. Yengo [a,1], Hüseyin Uysal [a,1], Robert Karlsson [b,2], Marjolein M.G.M. Thunnissen [a,*]

[a] Center for Molecular Protein Science, Lund University, Getingevägen 60, 221 00, Lund, Sweden
[b] GE Healthcare Biosciences AB, Rapsgatan 7, SE 75450 Uppsala, Sweden

ARTICLE INFO

Article history:
Received 14 August 2009
Received in revised form 20 September 2009
Accepted 22 September 2009
Available online 1 October 2009

Keywords:
WT1
Transcription factor
Zinc finger
Surface plasmon resonance
DNA-binding
Bacterial 1-hybrid system

ABSTRACT

Wilms Tumor suppressor protein (WT1) is a transcription factor that is involved in a variety of developmental functions during organ development. It is also implicated in the pathology of several different cancer forms. The protein contains four C_2H_2-type zinc fingers and it specifically binds GC-rich sequences in the promoter regions of its target genes, which are either up or down regulated. Two properties make WT1 a more unusual transcription factor — an unconventional amino acid composition for zinc finger 1, and the insertion of a tri-peptide KTS in some of the splice isoforms of WT1. Using six WT1 constructs in which zinc fingers are systematically deleted, a dual study based on a bacterial 1-hybrid system and surface plasmon resonance measurements is performed. The experiments show that the effect of zinc finger 1 is not significant in terms of overall DNA-binding kinetics, however it influences both the specificity of target recognition and stability of interaction in presence of KTS. The KTS insertion, however, only mildly retards binding affinity, mainly by affecting the on-rate. We suggest that the insertion disturbs zinc finger 4 from its binding frame, thus weakening the rate of target recognition. Finally, for the construct in which both zinc fingers 1 and 4 were deleted, the two middle fingers 2–3 still could function as a 'minimal DNA-recognition domain' for WT1, however the formation of a stable protein–DNA complex is impaired since the overall affinity was dramatically reduced mainly since the off-rate was severely affected.

1. Introduction

Wilms tumor is a child kidney malignancy that occurs with a frequency of 1:10000 [1]. In about 10% of the patient cases, mutations have occurred in the Wilms tumor suppressor gene (*WT1*). The *WT1* gene is located on the chromosome 11p13 and encodes a C_2H_2-type zinc finger protein (ZFP) that acts as a tumor suppressor [2,3]. The protein has a proline- and glutamine-rich regulatory domain (N-terminus) linked to a domain containing four zinc fingers of the Krûppel-type (C-terminus) [4,5]. In normal conditions WT1 regulates a vast network of genes during development of the kidney and the genitourinary system [2,3,6,7]. There is increasing evidence that WT1 also has an oncogenic role in a number of hematological malignancies and solid tumors, and this aspect is being exploited in cancer immunotherapies [8,9]. WT1 has over 20 known gene targets: some of these are activated while others are repressed. Some of these are identified as real target genes *in vivo* (see Supplementary Table 1). The mechanism that selects the targets and decides the type of regulation is not yet characterized, and is believed to depend on the cellular context [10,11]. It has been established that WT1 binds to the early growth response factor 1 (EGR1) consensus binding site 5′-GCG-(T/G)GG-GCG-3′. Subsequent studies have demonstrated a stronger binding to a series of longer sites summarized as 5′-GCG-(T/G)GG-GCG-(T/G)(A/G)(T/G)-3′ [12–14]. This 12-base pair site describes better the binding behavior of the four zinc fingers, where each ZF binds to a 3-base pair triplet [15]. Although there is a growing body of evidence showing that ZFPs, WT1 in particular, are capable of target regulation at the RNA level as well [16], no binding models and consensus sites have so far been characterized but recently the first cellular 34-basepair RNA target for WT1 ACT34 has been identified [17].

ZFPs are a class of regulatory proteins directly involved in a variety of cellular activities: among others development, differentiation and tumor suppression. Functionality of ZFPs is achieved through interacting specifically or non-specifically with DNA, RNA and even proteins. A zinc finger (ZF) is a small protein module with a special secondary structure stabilized by a zinc ion coordinated by Cys and His residues. Each ZF module can act independently in the course of DNA binding, although synergy between modules is also seen. Classification of ZFs depends on the different use of these residues

Abbreviations: B1H, Bacterial 1-Hybrid System; ZF, Zinc Finger; ZFP, Zinc Finger Protein; WT1, Wilms Tumor 1 Protein.

* Corresponding author. Tel.: +46 462224584; fax: +46 46 222 4116.
E-mail address: marjolein.thunnissen@mbfys.lu.se (M.M.G.M. Thunnissen).
[1] Tel.: +46 462224584; fax: +46 46 222 4116.
[2] Tel.: +46 18675764.

0301-4622/$ – see front matter © 2009 Elsevier B.V. All rights reserved.
doi:10.1016/j.bpc.2009.09.009

in zinc binding. WT1 belongs to the C_2H_2 class, which is mainly involved in transcription of target genes. [18] This category of ZFPs is estimated to comprise as much as 1% of total mammalian proteins.

Sequence alignment (Fig. 1) of the four ZFs of WT1 reveals that ZF1 differs substantially from the other three ZFs. Using a recognition code table based on the observation that the amino acids at positions −1, 2, 3, and 6 of the alpha helix within a ZF are responsible for determining the DNA-binding specificity [19], the DNA consensus sequence 5′-GCG-(T/G)GG-GCG-3′ could be determined to bind to ZFs 2-4 of WT1. However the amino acids found at the recognition positions in ZF1 are unconventional for ZFs and therefore no DNA sequence preference can be deduced with certainty for ZF1 using the recognition code table. In the search for a consensus for the binding site of ZF1, 28 potential WT1-binding sites from 12 human gene promoters were aligned. Although the results (Fig. 2) suggest that the binding site for ZF1 has a poor consensus sequence, guanine seems to be preferred at most of the triplet positions. Furthermore, some authors find evidence for a reduction in the DNA-binding activity of ZF1-deleted WT1 by as much as 90% in comparison to that of wild-type [14]. A role for ZF1 in RNA binding rather than DNA binding has also been proposed. A recent *in vivo* study on *Xenopus laevis* oocytes has reported that although both WT1 (+KTS) and WT1 (−KTS) were found bound to RNA transcripts, binding of a construct in which ZF1 was deleted was seriously weakened [16]. This suggests a probable involvement of ZF1 in locating and binding to RNA targets of WT1.

A second unusual aspect of WT1 is the translational/transcriptional regulation of the gene itself. Due to the existence of several different start-sites, alternative splice options and post-translational modifications, more than 24 isoforms of WT1 have been detected in mammals. The most common isoforms are the products of alternative splicing of the immature WT1 mRNA at exon 5 and exon 9, which produce 4 distinct isoforms with 17 and 3 amino acid insertions, respectively. The latter is of particular interest, since this encodes the KTS insertion into the linker between ZFs 3 and 4 which has been reported to decrease the binding to the DNA consensus sequence [5]. NMR experiments show that the KTS insertion relaxes the flexibility of the linker between ZFs 3 and 4, and may in fact reduce or abrogate binding of ZF 4 to its DNA targets [20]. On the other hand, the insertion of KTS differentially affects the affinity of WT1 for its single-stranded RNA targets — an interaction pattern, which is not yet understood [18,21].

Hence, the effects of the KTS insertion as well as the unconventional amino acid sequence within ZF1 on DNA, RNA and protein binding remain to be fully characterized. A wide spectrum of WT1 research is being conducted on biochemical, structural, immunological and cellular levels. The primary goal of a number of previously reported studies on WT1 kinetics has been to characterize the effects of various system conditions (pH, temperature, ionic strength etc.) on binding to different DNA [22] and RNA [21] targets. Despite this, there is as yet no accurate understanding of which ZFs undertake which specific roles in effective binding to the DNA and RNA targets in various physiological contexts.

In a previous study, the full-length C-terminal of WT1 was expressed and purified, and interactions between the −KTS and +KTS isoforms

```
                -1123456789
ZF1  FMCAYPGCNKRYFKLSHLQMHSRKHTGEKP
ZF2  YQCDFKDCERRFFRSDQLKRHQRRHTGVKP
ZF3  FQC——KTCQRKFSRSDHLKTHTRTHTGKTSEKP
ZF4  FSCRWPSCQKKFARSDELVRHHNMH
                  ***    *
```

Fig. 1. Alignment of the ZFs (1–4) of WT1. Numbers (−1 to 9) indicate amino acid positions within the α helices; highlighted positions are involved in specific binding to DNA. Asterisks are the amino acid positions significantly different in ZF1. Shown in bold are conserved cysteines and histidines, which coordinate Zn^{+2} ion. The *KTS* segment within the linker between ZF3 and ZF4 is the insertion that creates the two isoforms (WT1-KTS and WT1+KTS).

and the consensus DNA were observed using qualitative electrophoretic mobility shift assays [23]. Here, we report a dual study where, using six different truncations of the WT1 ZF domain, we attempt to describe the DNA-binding characteristics of WT1. In order to look at the DNA-binding site preferences of ZF1, a recently developed Bacterial 1-Hybrid System (B1H) [24] has been used. Subsequently, surface plasmon resonance studies (SPR), in which the various WT1 constructs were probed against DNA consensus sites, were performed. The technique is one of the newer methods used for assessment of DNA-binding kinetics; it has been applied successfully for analysis of protein–DNA interactions [22,25–32]. It enables extraction of the kinetics parameters k_{on} (association rate constant), k_{off} (dissociation rate constant) and K_D (equilibrium dissociation constant, $K_D = k_{off}/k_{on}$). Altogether, this data leads to a clearer and more robust understanding of the interactions between WT1 and DNA.

2. Materials and methods

2.1. Reagents and instrumentation

The chemicals used in B1H and SPR studies were of molecular biology grade and were purchased from Sigma (MO, USA). Restriction enzymes were purchased from New England Biolabs (Beverly, USA). Chemically synthesized DNA oligonucleotides were ordered from TAGC A/S (Copenhagen, Denmark). Components of the B1H system, reporter vector pH3U3, expression vector pB1H1 and the US0Δ*hisB*Δ*pyrF E. coli* selection strain, were a generous gift from University of Massachusetts Medical School. A BIACORE 3000 machine was used to perform all interaction assays. CM4 chip, EDC, NHS and ethanolamine were purchased from Biacore AB (Uppsala, Sweden). Streptavidin was from Pierce (IL, USA).

2.2. Cloning and purification of WT1 ZF truncations

Six different WT1 ZF truncations were generated for B1H and SPR studies: ZF14+, ZF14−, ZF24+, ZF24−, ZF13 and ZF23. The previously described constructs 6HIS-ZN+$_{wt1}$ and 6HIS-ZN−$_{wt1}$ were used as templates (Fig. 3, Table 1). The cloning steps, along with procedures for expression, purification and refolding of the proteins were as described previously [23]. For the purpose of the B1H study, the US0Δ*hisB*Δ*pyrF E. coli* selection strain was transformed with the ZF14− and ZF24− constructs. However, for the SPR measurements, the expressed proteins were further refolded, concentrated and transferred into the buffer containing 20 mM Tris–HCl pH 7.5 and 150 mM KCl, using a Superdex 75 gel filtration column. For all protein samples used in this study, the extinction coefficients were calculated individually according to Gill and Hippel [33] and the protein concentration was measured on a Lambda EZ210 spectrophotometer (PerkinElmer, USA) at a wavelength of 280 nm. Concentrations were additionally measured separately using Bradford [34] and micro Lowry methods [35]. After these procedures we obtained protein analytes with ≥95% purity.

2.3. B1H: design of binding site library

The binding site library was designed with a single oligonucleotide 5′-ATACATAGAT GCGGCCGC ATATA GCGTGGGCG NNNN ATATA GGCGCGCC ATAC-3′. Binding sub-sites for the WT1 ZFs 2–3–4 were kept constant, whereas a degenerate binding sub-site 5′-NNNN-3′ was provided for ZF 1. NotI and AscI restrictions sites were designed on the 5′- and 3′-end respectively, and 5′-ATATA-3′ spacers were provided to sufficiently expose the WT1 binding site and to separate it from the restriction sites. The library was extended with a primer 5′-GTATGGCGCGCCTATAT-3′ as described previously [36], and purified using the QIAquick nucleotide removal kit (Qiagen). The theoretical complexity of the library is calculated to be 256.

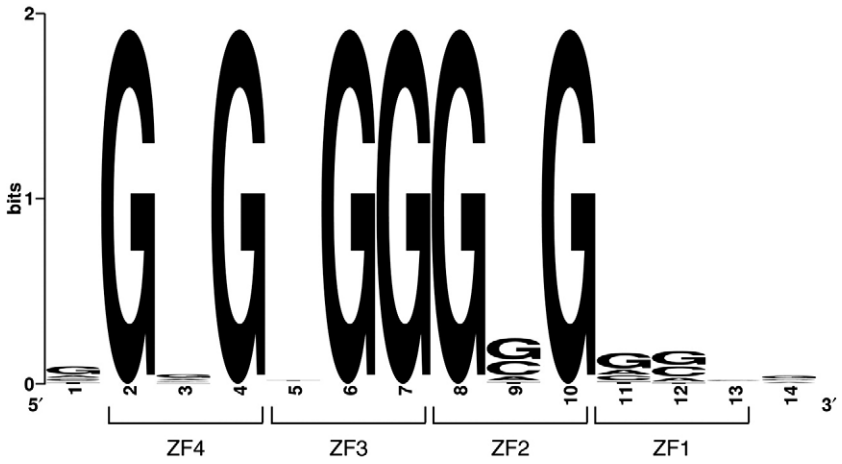

Fig. 2. Sequence logo obtained after alignment of 28 potential WT1 binding sites from 12 human gene promoters regulated by WT1. For the purpose of this alignment, −1500 segments of the coding strands of the promoters were searched for binding sites fitting the format 5′-N GNG NGG GNG NNN N-3′. The binding site for ZF1 (positions 11, 12, 13 and 14 from left) evidently has poor consensus, unlike the ones for ZF2–3–4 (positions 2 to 10). *Note*: The overall height of a stack indicates conservation at that position, while the height of symbols within the stack indicates the relative frequency of each nucleotide at that position. Lack of symbols indicates absence of conservation at a given position.

2.4. B1H: preparation of reporter constructs

The extended library and pH3U3 reporter vector were digested with NotI and AscI. The digested vector was gel-purified using a GenElute gel extraction kit (Sigma). The library was purified using a QIAquick nucleotide removal kit (Qiagen). The ligation reaction was optimized and performed as previously described [36]. The purified library was transfected into ElectroTen-Blue electroporation-competent *E. coli* cells (Stratagene); the library complexity was sufficient. This 'original' library was amplified and stored for further reference. To eliminate the self-ligated (empty) pH3U3 vector, we digested the 'original' library with restriction enzyme ApaLI, which cuts only in the region between the NotI and AscI restriction sites of intact vector. Electroporation-competent US0Δ*hisB*Δ*pyrF E. coli* selection strain was transformed with the gel-purified library with sufficient efficiency. The cells were processed, spread on 5-FOA (5-fluoro-orotic acid) plates to counter-select against self-activating binding sites, and cultivated — as described previously [36]. The numerous colonies were pooled together. This 'purified' library was extracted and stored for further reference.

2.5. B1H: binding site selection

Two separate lines of electroporation-competent US0Δ*hisB*Δ*pyrF E. coli* cells containing expression constructs ZF14— and ZF24— were transformed with the 'purified' binding site library. Transformation was performed in multiples to increase efficiency of library representation, as described previously [36]. Divided in equal aliquots, the cells were spread on 140 mm × 20 mm petri plates with various concentrations of 3-AT (3-amino-triazole) medium: 0 mM, 1.0 mM, 2.0 mM, 3.0 mM, 4.0 mM and 5.0 mM. Sealed plates were stored in the incubator at 37 °C for several days. Design of the B1H system is depicted in Fig. 4.

2.6. B1H: sequencing and analysis of binding sites

Fifteen random colonies from each plate were chosen for sequencing. Since the reporter vector is a low copy number plasmid, sequencing could not be made directly from the extracted plasmids. Using colonies as DNA templates, the region around the library insertion in the reporter vector was amplified with PCR using the primers:

5′-TGATCCCCTGCGCCATCAGATCCTTGGCGG-3′ and
5′-TACCTGTGTGGACGTTAATCACTTGCGATT-3′.

The binding sites were subsequently sequenced with the primer: 5′-CAAATATGTATCCGCTCATGAC-3′. The obtained binding sites were subjected to the MEME algorithm [37] for recognition of over-represented motifs. Sequence logos (Fig. 5) were generated for these sequences using the WebLogo server [38].

2.7. SPR: design of DNA duplexes

Five types of 5′-biotinylated DNA duplexes, BS1-5, were used in the SPR assays, as shown in Table 2. Complementary single DNA strands were mixed in equimolar amounts, heated to 95 °C for 5 min and cooled to room temperature to allow duplexes to form. Hybridized oligonucleotides were spun through G-25 (GE Healthcare, Sweden) columns to eliminate free biotin and nucleotides.

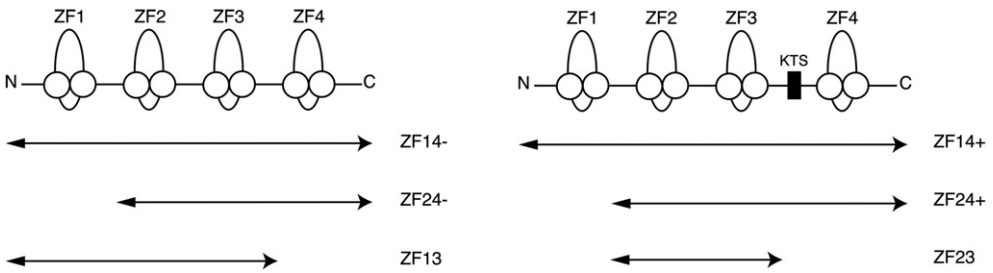

Fig. 3. WT1 ZF truncations generated via differential cloning. Arrow directions indicate the forward and reverse primers used for PCR. The number of zinc fingers inside each truncation should be deduced accordingly.

Table 1
Primers used for construction of the WT1 ZF truncations.

WT1 ZF truncations		Primers
B1H	ZF14−	Forward: 5′-GTACCAGTGAGAAACGCCCCTTCATGTGTGCTTA-3′ Reverse: 5′-GGATCCTCAAAGCGCCAGCTGGAGTTTGGT-3′
	ZF24−	Forward: 5′-GGTACCGGTGAGAAACCATACCAGTGTGACTTC-3 Reverse: 5′-GGATCCTCAAAGCGCCAGCTGGAGTTTGGT-3′
SPR	ZF14+, ZF14−	Forward: 5′-CCATGGAGAAACGCCCCTTCATGTGTGCTTA-3′ Reverse: 5′-CTATTTGGTCATGTTTCTCTGATGC-3′
	ZF24+, ZF24−	Forward: 5′-CCATGGAGAAACCATACCAGTGTGACTTC 3′ Reverse: 5′-CTATTTGGTCATGTTTCTCTGATGC-3′
	ZF13	Forward: 5′-CCATGGAGAAACGCCCCTTCATGTGTGCTTA-3′ Reverse: 5′-CTAACCTGTATGAGTCCTGGTGTGGGT-3′
	ZF23	Forward: 5′-CCATGGAGAAACCATACCAGTGTGACTTC 3′ Reverse: 5′-CTAACCTGTATGAGTCCTGGTGTGGGT-3′

The truncations are named ZF14+, ZF14−, ZF24+, ZF24−, ZF13 and ZF23. Presence and absence of the KTS insertion in the truncations is symbolized with '+' and '−', respectively. In the case of B1H constructs, the forward primers introduced the initial Methionine and a KpnI restriction site, whereas the reverse primer introduced a BamHI restriction site downstream of the stop codon. The DNA fragments cloned into the expression vector pB1H1 were sequenced with primer 5′-GATTCGTCGTGCGGCAACCA-3′.

2.8. SPR measurements

The 'kinetic titration series' approach [39] was chosen for data collection. Hence, different concentrations of analyte were injected over the chip surface in five consecutive injections without regeneration. A CM4 chip surface was activated with a mixture of NHS (0.05 M) and EDC (0.2 M). Immobilization was performed at a flow rate of 30 µl/min in 20 mM Hepes pH 7.4, 150 mM KCl and 0.005% P20 surfactant. Streptavidin was injected at a concentration of approximately 50 µg/ml in 10 mM sodium acetate pH 4.0. Ethanolamine (1 M, pH 8.5) was injected to quench remaining active groups. An average of 3000 RU of streptavidin was immobilized on each flow cell. Biotinylated DNA duplexes in concentration of 50 nM were injected until a desired immobilization level of 100–300 RU was achieved. A streptavidin-immobilized and ethanolamine-blocked flow cell, usually 1 and/or 3, was used as reference. A random DNA sequence was used as a control for specificity of interaction (Table 2).

SPR assays were performed at 25 °C using a running buffer with 20 mM Tris–HCl pH 7.5, 150 mM KCl, 1 mM $MgCl_2$, 1 mM DTT and 0.005% (v/v) surfactant P20. After the last gel filtration step, all of the six protein samples were concentrated and stored at −80 °C until used. All the protein samples were diluted in running buffer containing 1 mg/ml carboxymethyl (CM) dextran. All the dilutions used for the measurements were made from the same sample stock to eliminate any possible concentration errors.

Initially, running buffer was administered in 5 injections to account for the effect of buffer signal and to assess baseline behavior. The flow rate was maintained at 30 µl/min. Dilution factor ($F=2$) and concentration (*CONC*) of each analyte was carefully chosen. Sequentially increasing concentrations of the analytes were flown over the DNA-immobilized surface at a flow rate of 30 µl/min. The analytes were assayed on the immobilized DNA ligands according to the combinations given in Table 2.

To obtain the final data, interaction curves were subjected to subtraction of references and correction by blanks for instrument drift and refractive index changes (Fig. 6, Supplementary Fig. 1). The previously reported algorithm used for the evaluation of 'kinetic titration series'-type data [39] was modified to include the effect of drift, since this effect could not be completely eliminated. The modified algorithm was incorporated into the BIA Evaluation version 4.1 (Biacore AB), and curve fitting was performed assuming a 1:1 Langmuir interaction. Selection of defaults and initial values for the parameters in the model were as set formerly [39]. However, initial values for k_{on}, k_{off} and k_t (coefficient for drift) were entered as 10^5, 10^{-3} and 5×10^8, respectively.

3. Results

3.1. B1H study

The purpose of the B1H analysis was to investigate a possible sequence preference of the binding sub-site for WT1 ZF1 (Fig. 4). The segments of WT1 (−KTS) ZF domain encoding ZF14− and ZF24− were separately fused to the α-subunit of RNA polymerase in the expression vector, as described above. When the ZFs are engaged in productive binding with a member of the WT1 binding site library located upstream of a weak promoter in the reporter vector, the fused RNA polymerase is recruited to activate transcription of the reporter genes *HIS3* and *URA3*. Colonies that appear on high stringencies (high 3-AT concentration) are products of a strong interaction, whereas those that appear on lower stringencies can have weaker interactions. The three sets of selections used in this study are described in Table 3.

The efficiency of selection in 5-FOA and 3-AT media was calculated to be around 5×10^7 transformants, which is sufficient to represent a library with a complexity of 256 (4^4) variants. Colonies appeared in the course of 2–4 days. The number of colonies obtained at various stringencies is shown in Table 3. In control 1, cells were able to survive at maximum 2 mM 3-AT. In control 2, colonies appeared at maximum 4 mM 3-AT. In comparison to the two controls, survival ability of Lib-ZF14− cells was raised to 5 mM 3-AT. It is evident that the presence of ZF1, which is absent in control 2, causes colony survival at stringencies even greater than 4 mM 3-AT.

Fifteen Lib-ZF14− colonies from each stringency between 2 and 5 mM were randomly selected and sequenced. The obtained ZF1 binding site logos for the various stringencies are shown in Fig. 5. At

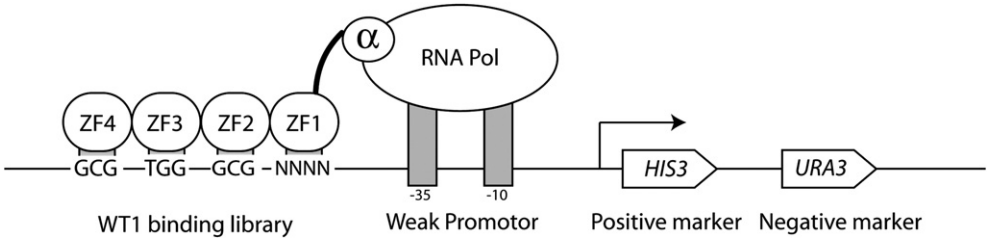

Fig. 4. Schematic illustration of the B1H system. The ZF domain (bait) of WT1 is fused to the alpha-subunit of RNA polymerase in the expression vector. A library of randomized DNA-binding sub-sites, 5′-NNNN-3′, (prey) is inserted upstream of *HIS3* and *URA3* genes in the reporter vector. Binding sub-sites for the ZFs 2–3–4 are kept stable for anchoring. Interaction of ZFs with the target sequences will recruit the fused RNA polymerase to activate the two reporter genes. Contribution from binding of ZF1 will add strength to the interaction.

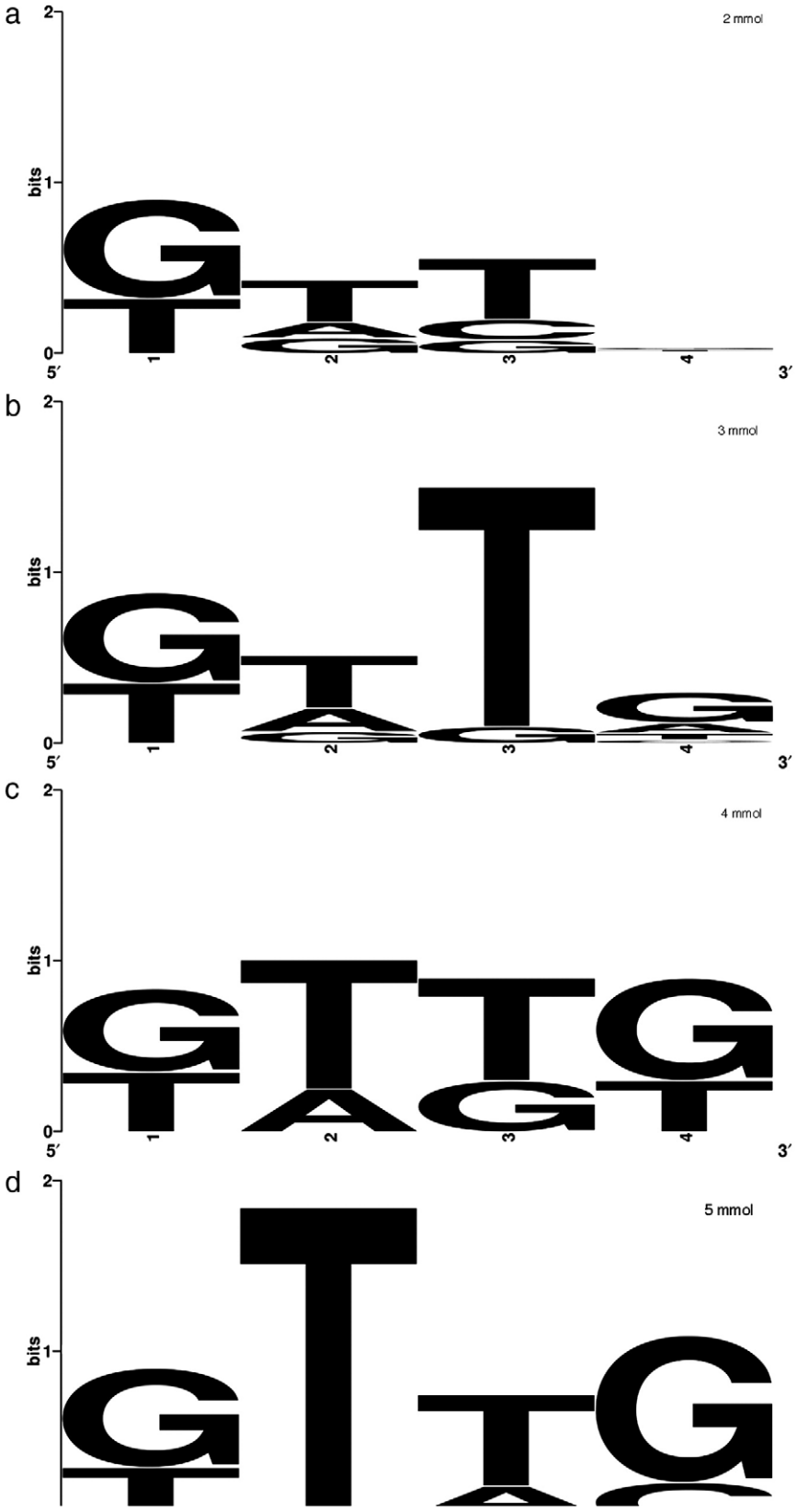

Fig. 5. Binding site motifs obtained various stringencies, 2.0, 3.0, 4.0 and 5.0 mM 3-AT. Each motif was obtained through alignment of fifteen over-represented sequence motifs. Even though GTTG is the strongest represented target of ZF1 at the highest stringency, its tolerance to other sequences becomes apparent at lower stringencies.

5 mM 3-AT, ZF14— shows a clear preference for a binding site dominated by GTTG. While each of the nucleotide positions 1, 3 and 4 allowed a second recessive possibility, position 2 was found to be a strongly conserved thymine. At 4 mM 3-AT, the binding site was still represented by GTTG, however, at position 2 also a comparably weaker adenine is tolerated. Even though the binding pattern at 3 mM 3-AT was still dominated by GTTG, the strict requirement for a T or a G respectively at positions 2 and 4 were considerably reduced. Finally,

Table 2

(A) Desciption of the ligands designed for the SPR measurements.

DNA ligand	Sequence
BS1	5′-TCATTACAAT*GCGTGGGCGGGG*AATCTT ACTA-3′ 3′-AGTAATGTTACGCACCCGCCCCTTAGAA TGAT-biotin-5′
BS2	5′-TCATTACAAT*GCGTGGGCG*AATCTTACTA-3′ 3′-AGTAATGTTACGCACCCGCTTAGAATGAT-biotin-5′
BS3	5′-TCATTACAAT*TGGGCGGGG*AATCTTACTA-3′ 3′-AGTAATGTTATCCCGCCCCTTAGAATGAT-biotin-5′
BS4	5′-TCATTACAAT*GCGTGGGCGGTTG*AATCTTACTA-3′ 3′-AGTAATGTTACGCACCCGCCAACTTAGAATGAT-biotin-5′
BS5	5′-TCATTACAAT*TGGGCGGTTG*AATCTTACTA-3′ 3′-AGTAATGTTAACCCGCCAACTTAGAATGAT-biotin-5′
Control	5′-CTAGTGTTAATACCATAATGCAGAAACAGA-3′ 3′-GATCACAATTATGGTATTACGTCTTTGTCT-biotin-5′

(B) Description of the analyte–ligand combinations assayed in the study.

Ligand : Analyte	Description
BS1 : ZF14− and ZF14+	Binding sites for all four ZFs are provided. ZF1 binds to GGG — extracted from promoter sequence analysis.
BS2 : ZF24− and ZF24+	Binding sites for ZFs 2–4 are provided.
BS3 : ZF13 and ZF23	Binding sites for ZFs 1–3 are provided. ZF1 binds to GGG — extracted from promoter sequence analysis. Test for 'minimal DNA-recognition domain'.
BS4 : ZF14− and ZF14+	Binding sites for all four ZFs are provided. ZF1 binds to GTTG — extracted from B1H system.
BS5 : ZF13 and ZF23	Binding sites for ZFs 1–3 are provided. ZF1 binds to GTTG — extracted from B1H system. Test for 'minimal DNA-recognition domain'.
Control : ZF14− and ZF14+	Accounts for binding affinity to a non-consensus DNA sequence

The consensus sites are shown in italics. The length of the spacers on either side of each binding site was designed to maximally expose the binding sites on the chip surface for unbiased interactions. The content of the spacers was arbitrarily chosen to be GC-poor. Control sequence is randomly chosen to be completely dissimilar from the consensus site.

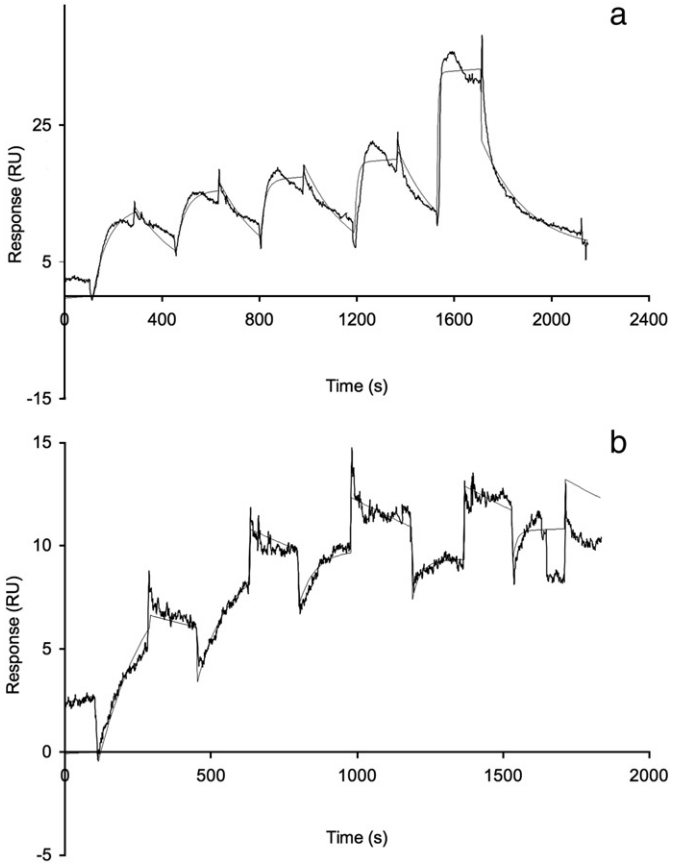

Fig. 6. Two kinetic titration sensorgrams of a pair of WT1 ZF truncations. Each sensorgram contains five sequential analyte injections with increasing concentration, from left to right. The highest analyte concentrations (*CONC*) are indicated in brackets. The dilution factor (*F*) used throughout the measurements is 2. Refer to Table 4 for the derived kinetic data. a) BS4: ZF14− (375 nM), chi^2 is 3. b) BS4: ZF14+ (750 nM), chi^2 is 0.5. Sensorgrams for the remaining measurements are provided in Supplementary Figs. 1 and 2.

the binding pattern GTTG was not dominant at 2 mM 3-AT, although guanine still prevailed at position 1 and thymine dominated at positions 2 and 3. The nature of the base at position 4 had apparently no significance at the lowest stringency.

3.2. SPR studies

Studies using SPR need to be fine-tuned according to the nature of the analytes and ligands, the biochemistry of their interaction and the questions to be answered. Matching the WT1 ZF truncations with particular DNA ligands (Table 2) ensured that each ZF binds to only its high-specificity DNA triplet and no subsequent shifts occur within the binding frame that produce aberrant binding patterns. The expected interaction pattern, based on an anti-parallel alignment of the ZF polypeptide and the DNA chain, is as depicted in Fig. 7A.

Due to their specific biophysical nature (i.e. p$I > 10$), the analytes were positively charged in the assay buffers at pH 7.5. Therefore, in order to eliminate unspecific binding of the ligands to the negatively charged carboxymethylated dextran on the chip surface, CM dextran sodium salt was added to the analyte dilution buffer to a final concentration of 1 mg/ml, which was empirically determined. At this minimal concentration CM dextran competes with the charged sensor surface without itself introducing non-specific interactions with the analyte. The initial concentration of the injected analyte was subsequently optimized to give a good and reproducible signal over noise.

The sensorgrams obtained after reference subtraction are summarized in Fig. 6 and Supplementary Fig. 1. Technical problems related to mass transfer and steric hindrance were eliminated through increasing the flow rate to 30 µl/min and using a low immobilization level of DNA (only 100–300 RU). The classical method of data collection (several single injections at various analyte concentrations) was not used since this led to poor regeneration of the chip surface. Instead a kinetic titration series approach was used instead since this circumvented the need for regeneration after every injection. Fitting of the saw-tooth-pattern sensorgrams yielded typically chi^2 (goodness of fit) values below 10, indicating reliable quality of fitting. Measurements obtained for each type of interaction were averaged,

Table 3
Description of the samples used in the B1H study, and numbers of colonies obtained at various concentrations of 3-AT.

Description	Lib-ZF14- ZF14- interacts with the complete binding site library.	No-Lib-ZF14-*(Control 1)* ZF14- interacts with an empty reporter vector (i.e. no binding site library).	Lib-ZF24-*(Control 2)* ZF24- interacts with the complete binding site library.
Stringency		Colony numbers	
0 mM	>6000	>6000	~6000
1.0 mM	~5100	4	102
2.0 mM	~4000	2	57
3.0 mM	140	0	35
4.0 mM	86	0	2
5.0 mM	65	0	0

Control 1 gave an estimate of survival level without involvement of the desired interaction between ZF domain and the binding site library. Control 2 revealed the threshold of survival accounted for interaction between the library and ZFs 2–3–4 only. Thus, Lib-ZF14− survivors on the stringencies higher than those found for the two controls would be attributed primarily to the interaction of ZF1 with its binding subsites from the library. All samples were treated similarly throughout the study.

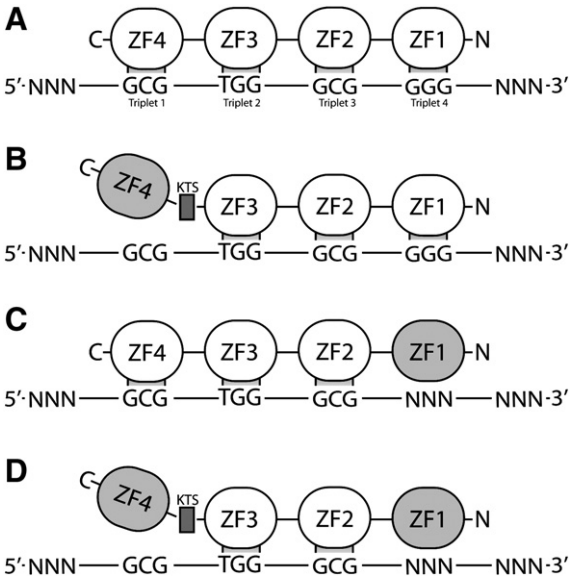

Fig. 7. Cartoon representing the interaction of WT1 ZFs with DNA. (A) Classical situation where each ZF binds to its target sub-site; (B) Displacement of ZF4's binding frame due to KTS; (C) Unspecific binding of ZF1; (D) A situation with both B and C, where ZF2–3 acts as the minimal DNA-recognition domain.

and errors were subsequently estimated for each interaction from the variations within the data sets (Table 4).

To investigate the role of the different ZFs and the KTS insertion, six different constructs were made and twinned studies were performed to investigate the role of the individual components. To investigate a probable role of ZF1 in binding of WT1 to DNA, two sets of sub-sites were selected: 1) GGG was selected from the promoter sequence alignments (Fig. 2), and 2) GTTG was selected from the *in vivo* B1H analysis (Fig. 5). Data obtained from the measurements is summarized in Table 4 and sketched in Fig. 7C.

Our data indicate that the presence of ZF1 did not significantly change the kinetic behavior of the protein in respect to DNA binding. When comparing BS1:ZF14− and BS2:ZF24− (Table 4), it can be seen that the overall binding affinity was not affected since both the on- and off-rates are decreased by one order of magnitude. Likewise, when comparing BS4:ZF14− and BS2:ZF24−, the absence of ZF1 again equally affects both on-rates and off-rates, thereby not changing the overall affinity.

The effect of the KTS tri-peptide insert between ZF3 and ZF4, i.e., in the middle of the canonical linker TGEKP, has been reported to be the abrogation of binding to DNA [5]. However, a comparison of the kinetics of BS1:ZF14− and BS1:ZF14+ (Table 4) indicates that the presence of the KTS element did not decrease the affinity to DNA. The same behavior is observed when the interactions of BS4:ZF14− and BS4:ZF14+ are compared. Also in this case the affinity for the latter did not decrease. However, when the interactions of BS2:ZF24− and BS2:ZF24+ are compared, there is a 6-fold reduction in affinity. The KTS-induced decrease in affinity of ZF24+ was fully accounted for a slower k_{on}, while k_{off} remained unaffected. It implies that KTS retards recognition of the target DNA approximately by a factor of 5. However, once bound, it takes equal time for ZF24− and ZF24+ to leave the target. Involvement of KTS is sketched in Fig. 7B.

Table 4
Kinetic data of the six WT1 ZF truncations, as indicated in Table 2B.

Interaction	k_{on} (M^{-1} s^{-1})	k_{off} (s^{-1})	K_D (k_{off}/k_{on}) (M)
BS1 : ZF14−	$(1.12\pm0.23)\times10^{5}$	$(6.1\pm0.7)\times10^{-4}$	$(5.5\pm1.1)\times10^{-9}$
BS1 : ZF14+	$(3.61\pm0.96)\times10^{5}$	$(6.34\pm1.6)\times10^{-4}$	$(1.77\pm1.31)\times10^{-9}$
BS2 : ZF24−	$(1.15\pm0.05)\times10^{6}$	$(4.94\pm0.9)\times10^{-3}$	$(4.31\pm0.93)\times10^{-9}$
BS2 : ZF24+	$(2.35\pm0.4)\times10^{5}$	$(5.92\pm0.27)\times10^{-3}$	$(2.53\pm0.87)\times10^{-8}$
BS3 : ZF13	$(2.45\pm0.29)\times10^{5}$	$(4.45\pm0.44)\times10^{-3}$	$(1.80\pm0.39)\times10^{-8}$
BS3 : ZF23	$(4.65\pm0.13)\times10^{5}$	$(1.44\pm0.87)\times10^{-1}$	$(3.11\pm0.4)\times10^{-7}$
BS4 : ZF14−	$(4.93\pm0.91)\times10^{5}$	$(4.84\pm0.71)\times10^{-3}$	$(9.83\pm0.97)\times10^{-9}$
BS4 : ZF14+	$(2.20\pm0.1)\times10^{5}$	$(1.63\pm0.13)\times10^{-3}$	$(7.36\pm0.24)\times10^{-9}$
BS5 : ZF13	$(1.57\pm0.22)\times10^{6}$	$(2.69\pm0.17)\times10^{-2}$	$(1.74\pm0.16)\times10^{-8}$
BS5 : ZF23	$(1.38\pm0.04)\times10^{5}$	$(1.17\pm0.2)\times10^{-1}$	$(8.51\pm1.16)\times10^{-7}$
Control : ZF14−	–	–	–
Control : ZF14+	–	–	–

Curves of these interactions are provided in Fig. 6 and Supplementary data. Curves of control measurements are provided in Supplementary data.

To estimate the contribution of ZF4, the kinetics for BS1:ZF14− and BS3:ZF13 are compared. From these data there is a clear indication of the direct kinetic contribution of ZF4 without any influence of KTS. In the case of ZF13 (no ZF4 present), affinity is reduced by 3-fold. Similarly, if BS4:ZF14− and BS5:ZF13 are compared, a 2-fold reduction in affinity can be observed. Its effect is more pronounced on the off-rates. Thus, regardless to which target sub-site ZF1 bound (GGG vs. GTTG), the effect of ZF4 was notable. Therefore, it seems that ZF4 plays a crucial role in functionality of WT1 as a transcription factor.

To assess the possibility of the two middle zinc fingers functioning as the sole DNA-recognition domain (see Fig. 7D), a WT1 variant, ZF23 was generated in which both ZF1 and ZF4 were deleted. The affinity of ZF23 to BS3 or BS5 is on the 10^{-7} level. By comparing both BS1:ZF14− vs BS3:ZF23 and BS4:ZF14− vs BS5:ZF23, it can be seen that mainly the off-rates were dramatically affected, while the on-rate stayed largely unaffected. In other words, ZF23 cannot remain bound to DNA sufficiently. This highlights the fact that ZF4 contributes significantly to the stabilization of the interactions of WT1 with its DNA target. Therefore, while this data does support the possibility for ZF2-3 functioning as a minimal DNA-recognition domain for WT1, the formation of a stable complex will be impaired.

4. Discussion

We conducted a dual study of the DNA-binding behavior of WT1, using both a B1H system and SPR measurements using different truncations of the ZF domain of WT1. ZF domains on their own have been successfully used in DNA-binding experiments without the functional domains with which they appear in the cell [40,41]. Even though synergy exists between neighboring ZF modules in a protein, each module can potentially bind to DNA as an independent unit [19,42–44], as sketched in Fig. 7A. Thanks to this inherent feature, various types of studies have been possible, where ZFs are truncated [45–49], 'switched off' [50], swapped [51,52], recombined [51] or fused [53]. Therefore we believe that the six protein analytes used in our investigation retained their wild-type DNA-binding properties. In electrophoretic mobility shift assays it has been seen that the DNA-binding capacity of the C-terminal domain is retained in the absence of the N-terminal domain [23].

The SPR measurements were performed with an addition of 1 mg/ml CM dextran sodium salt in order to avoid unspecific binding of the analytes. CM dextran salt is used in more complex samples such as cell lysates and serum to reduce binding of unwanted components and the effect on analyte binding is controlled by adding varying amounts of analyte to the sample and by looking at the recovery. In the ideal case analyte binding is only marginally affected. In this case, as the analyte binds to the soluble CM dextran salt, the question is how much of the concentration of the analyte that can bind to the immobilized ligand is reduced. By using a 1:1 Langmuir fitting model, the concentration of the analyte might be overestimated thus leading to k_{on} being underestimated. However this has no effect on k_{off} as this is concentration-independent. Since this study is mainly comparative and a concentration series of the analyte is used, we believe that our strategy to use the simple fitting method is justifiable as this avoids statistical over-fitting of the obtained curves. The obtained kinetic values in our study are in accordance with data reported for similar systems. The SPR measurements show that WT1

is a strong DNA-binding transcription factor that operates with an affinity in 10^{-9} M-range, in accordance with the figure of 1.14×10^{-9} M reported previously (Table 4, Fig. 6, Supplementary Fig. 1) [54]. The specificity of the interaction is clear if one compares this to the data of the control DNA (Supplementary Fig. 2), to which WT1 fails to bind.

The main interest of the study was to investigate the role of the KTS insert in specific WT1 isoforms as well as a putative role for ZF1. The KTS insert has been studied extensively and the specific role of the insert in the protein behavior has been debated. One theory puts forward that the KTS insert displaces ZF4 such that the critical DNA-binding amino acids cannot reach the GCG sub-site and the tight interactions are disrupted (see Fig. 7B). The possibility of such a displacement is supported by a study where KTS is found to increase the linker flexibility and weaken DNA binding by ZF4 [20]. In another study it was proposed that the KTS insertion disrupts the α-helices in ZFs 3 and 4, probably caused by destabilization of the DNA-induced C-capping motifs in ZF3 [55]. Conflicting reports have been published since binding to DNA of a WT+KTS variant has been observed in electrophoretic mobility shift assays [23], and mice that only express the KTS+ or KTS− variants of the protein are viable while full WT1 knock-out mice die at mid-gestation [56]. Thus an overlap in functioning of the two isoforms including DNA binding must be present. Furthermore a DNA-binding site and a transcriptional target has been observed for the fusion protein EWS–WT1(+KTS) (a fusion between the N-terminal domain of the Ewing's sarcoma gene EWS and ZFs 2 to 4 of WT1 with the presence of the alternative splice site leading to a +KTS and a −KTS variant) [57]. Both isoforms of EWS–WT1 can transcriptionally activate *ENT4* (equilibrative nucleoside transporter 4) with the +KTS form being the more effective one [58].

When the influence of the KTS insert was investigated using SPR measurements, no severe reduction in affinity between ZF14− and ZF14+ was observed. The KTS insert does influence DNA binding more when different constructs are compared like BS2:ZF24− and BS2:ZF24+ (where ZF1 is absent). Here the overall affinity is reduced 6-fold in the presence of KTS caused by a significantly retarded on-rate. This observation suggests a possibility that the KTS insert only mildly disturbs ZF4 from its binding frame without seriously altering the nature of DNA binding itself and the interaction process is only affected at the recognition stage. These data show that indeed the +KTS variant can complex with DNA in a simplified model system. Whether the full WT1 (+KTS) also can bind DNA directly within the cellular context remains unclear. Here, interactions with other factors (like other regulatory proteins), and the changed pattern of cell-location play an important role.

The significance of ZF4 itself can be assessed by comparing BS1:ZF14− vs. BS3:ZF13 and BS4:ZF14− vs. BS5:ZF13. The absence of ZF4 reduced the affinity 3-fold and 2-fold, respectively, caused mainly by a retarded k_{off} (7- and 6-fold, respectively), while k_{on} remained unaffected. The difference in k_{off} demonstrates that ZF4 enhances the ability of WT1 to form a stable complex with DNA and the extra contacts provided by ZF4 contribute effectively to the DNA–protein interaction strength. Thus, the extra 3-bp DNA contacts provided by ZF4 increase the specificity of binding to a DNA target 64-fold. On the molecular level this implies a more efficient target locating ability and higher specificity.

The interplay between KTS and ZF4 might be a potential source for enhancement of the sequence recognition potential of WT1. The KTS moiety might give WT1 flexibility to reach target sequences with interrupted binding sub-sites. Furthermore the KTS insertion might be more significant in RNA binding even though these interactions are not well understood. KTS differentially affects the affinity of WT1 for its single-stranded RNA targets [18,21]. Single-stranded RNA has more conformational freedom than double-stranded DNA and can have a well-defined three-dimensional structure. The insertion of KTS might therefore direct ZF4 to a different part of the three-dimensional RNA structure.

The role of ZF1 in DNA binding seems to be minimal. The presence of ZF1 increased the capacity of cells to tolerate 3-AT at considerably higher stringencies in the BH1 studies. Therefore, the presence of ZF1 seems to be beneficial for complex formation between WT1 and DNA. However the binding seems not to be governed by a specific sequence at lower stringencies and only at higher stringencies a sequence represented by GTTG seems to be the preferred binding sub-site. Interestingly, comparison of this weak consensus site to the ZF1 binding sites from WT1's *bona fide* target genes (see Supplementary Table 1) revealed poor similarity. Therefore, it seems that under true physiological conditions the contributions of ZF1 to DNA binding are of a rather unspecific nature in comparison to the specifically directed interactions the other ZFs make and only under very stringent conditions a preference can be detected.

These subsequent studies showed that involvement of ZF1 in DNA binding is not significant in terms of kinetics, even though both association and dissociation rates are affected, the overall affinity remains mostly unchanged (BS1:ZF14− vs. BS2:ZF24−). This is in agreement with a recent structural study, where ZF1 is seen to align itself in the DNA major groove and interact with the phosphodiester backbone, without making essential base-specific contacts [59]. Its deletion affects binding kinetics insignificantly, hence pointing at its secondary role in DNA binding [13,14,60]. However, according to our investigation, the effect of ZF1 is more pronounced when KTS is inserted (BS1:ZF14+ vs. BS2:ZF24+), further complicating its role. An influence of ZF1 in DNA binding could be modulating the specificity of the other 3 ZFs indirectly as suggested from studies of the fusion protein EWS–WT1(−KTS). This protein lacks the first zinc finger and this might account for the distinct DNA binding specificity *in vivo* of this fusion protein compared to native WT1 [61]. Therefore, interplay between ZF1 and KTS as well as effect of ZF1 on DNA binding could greatly depend on the cellular context especially in view of the fact that other protein factors are known to modulate WT1 function [11].

Interestingly in the B1H experiments, judging from the colony counts of Lib-ZF14− and Lib-ZF24−, the presence of ZF1 is significant for cell survival (Table 3). In the case of Lib-ZF24−, the number of colonies is drastically decreased from 6000 to 102 when subjected to high stringency. In contrast, the number of colonies of Lib-ZF14− is not as much affected. However, this is not reflected in the SPR measurements that were performed with a ligand that contained the observed recognition GTTG sequence. No main differences are observed when the different constructs and ligands are compared; BS1:ZF14− vs. BS4:ZF14−, BS1:ZF14+ vs. BS4:ZF14+, or BS3:ZF13 vs. BS5:ZF13 (Table 4). These *in vitro* experiments seem not to be sufficient to reflect the complex molecular environment of a cell, where ZF1 might interact with various protein and RNA partners and more subtle benefits of ZF1 can be established. Also the influence of the full WT1 protein has to be taken in account. For example, it is known that the full-length protein is able to dimerise [61] and thus there might be interplay between ZF1 and its N-terminal domain. ZF1 is reported to play a more important role in RNA recognition, and its presence there plays a major role [16] and it appears that it behaves in a context-dependent manner and some synergy can be seen in the presence of the KTS insertion. This might be a mechanism of fine-tuning the binding kinetics for the myriad targets of WT1, whose kinetically differential selection is a necessity, if one considers the complexity of WT1 biology.

It has been suggested that the transcriptional affinity and specificity of protein–DNA interactions are mainly dictated by dissociation rates, as even non-specific partners may associate due to attracting electrostatic forces. However, specific gene regulators associate with their targets much more tightly, with slow dissociation rates. A study with several variants of Adr1 has shown its *in vivo* activity to depend mostly on k_{off}, rather than on k_{on} or K_D. For a gene to be activated by Adr1, accessibility to the binding site *in vivo* is not the rate-limiting step [30,41]. Albeit uncommon, there are several

naturally occurring two-ZF proteins like Tramtrack, which was found to bind specifically to an 11-bp DNA sequence with a K_D of 4×10^{-7} M [62]. Another similar domain with two ZFs from human enhancer binding protein, MBP1 has been found to specifically recognize a 15-bp sequence with a K_D of 1.4×10^{-7} M [63]. A third unrelated protein, ADR1, binds several of its targets with K_D values varying in the range of 6.4×10^{-8}–5.70×10^{-7} M [41]. These values are in the same order of magnitude as the K_D values we measured for ZF23 (Fig. 7D), 8.51×10^{-7} M and 3.11×10^{-7} M for BS5 and BS3, respectively. These values are dominated by k_{on} ($10^5\,M^{-1}s^{-1}$-level), whereas the contribution by k_{off} is relatively insignificant ($10^{-1}\,s^{-1}$-level). This indicates that although the ZF23 is able to recognize DNA, its ability to form a stable complex is impaired as compared with the full C-terminal domain.

To summarize, this dual study provides new insights into the DNA-binding behavior of the different isoforms of WT1. Using an *in vivo* B1H system, we show that ZF1 seems to interact unspecifically with a range of DNA sequences; and we believe it functions in a cellular context-dependent manner. ZF4 significantly contributes to target locating capability of WT1 with its strong DNA contacts. The KTS insertion only mildly disturbs WT1 from its binding frame, thus only a limiting reduction of DNA-binding affinity could be measured. Finally, we conclude that the middle two ZFs of WT1 can act as a minimal DNA-recognition domain although the complex with DNA will have lower stability.

Acknowledgements

We are grateful to Biacore AB (Uppsala, Sweden) for providing professional assistance with the SPR measurements. We also acknowledge Cancerfonden (CAN 2007/1020 Sweden) and Vetenskapsrådet (Sweden) for financing this research. Last but not least, we owe thanks to Dr. Derek Logan for proofreading this manuscript.

Appendix A. Supplementary data

Supplementary data associated with this article can be found, in the online version, at doi:10.1016/j.bpc.2009.09.009.

References

[1] E. Matsunaga, Genetics of Wilms' tumor, Hum. Genet. 57 (1981) 231–246.
[2] K.M. Call, T. Glaser, C.Y. Ito, A.J. Buckler, J. Pelletier, et al., Isolation and characterization of a zinc finger polypeptide gene at the human chromosome 11 Wilms' tumor locus, Cell 60 (1990) 509–520.
[3] M. Gessler, A. Poustka, W. Cavenee, R.L. Neve, S.H. Orkin, et al., Homozygous deletion in Wilms tumours of a zinc-finger gene identified by chromosome jumping, Nature 343 (1990) 774–778.
[4] S.L. Madden, D.M. Cook, J.F. Morris, A. Gashler, V.P. Sukhatme, et al., Transcriptional repression mediated by the WT1 Wilms tumor gene product, Science 253 (1991) 1550–1553.
[5] F.J. Rauscher III, J.F. Morris, O.E. Tournay, D.M. Cook, T. Curran, Binding of the Wilms' tumor locus zinc finger protein to the EGR-1 consensus sequence, Science 250 (1990) 1259–1262.
[6] A. Huang, C.E. Campbell, L. Bonetta, M.S. McAndrews-Hill, S. Chilton-MacNeill, et al., Tissue, developmental, and tumor-specific expression of divergent transcripts in Wilms tumor, Science 250 (1990) 991–994.
[7] J. Pelletier, M. Schalling, A.J. Buckler, A. Rogers, D.A. Haber, et al., Expression of the Wilms' tumor gene WT1 in the murine urogenital system, Genes Dev. 5 (1991) 1345–1356.
[8] Y. Oka, I. Kawase, Cancer antigen WT1-targeting treatment for the malignancies, Nihon Rinsho Meneki Gakkai Kaishi 31 (2008) 375–382.
[9] C. Chaise, S.L. Buchan, J. Rice, J. Marquet, H. Rouard, et al., DNA vaccination induces WT1-specific T-cell responses with potential clinical relevance, Blood 112 (2008) 2956–2964.
[10] A. Menke, L. McInnes, N.D. Hastie, A. Schedl, The Wilms' tumor suppressor WT1: approaches to gene function, Kidney Int. 53 (1998) 1512–1518.
[11] S.B. Lee, D.A. Haber, Wilms tumor and the WT1 gene, Exp. Cell Res. 264 (2001) 74–99.
[12] F. Borel, K.C. Barilla, T.B. Hamilton, M. Iskandar, P.J. Romaniuk, Effects of Denys–Drash syndrome point mutations on the DNA binding activity of the Wilms' tumor suppressor protein WT1, Biochemistry 35 (1996) 12070–12076.
[13] T.B. Hamilton, K.C. Barilla, P.J. Romaniuk, High affinity binding sites for the Wilms' tumour suppressor protein WT1, Nucleic Acids Res. 23 (1995) 277–284.
[14] H. Nakagama, G. Heinrich, J. Pelletier, D.E. Housman, Sequence and structural requirements for high-affinity DNA binding by the WT1 gene product, Mol. Cell. Biol. 15 (1995) 1489–1498.
[15] N.P. Pavletich, C.O. Pabo, Zinc finger–DNA recognition: crystal structure of a Zif268–DNA complex at 2.1 A, Science 252 (1991) 809–817.
[16] M. Ladomery, J. Sommerville, S. Woolner, J. Slight, N. Hastie, Expression in Xenopus oocytes shows that WT1 binds transcripts in vivo, with a central role for zinc finger one, J. Cell Sci. 116 (2003) 1539–1549.
[17] A.A. Morrison, J.P. Venables, G. Dellaire, M.R. Ladomery, The Wilms tumour suppressor protein WT1 (+KTS isoform) binds alpha-actinin 1 mRNA via its zinc-finger domain, Biochem. Cell Biol. 84 (2006) 789–798.
[18] S. Iuchi, Three classes of C2H2 zinc finger proteins, Cell. Mol. Life Sci. 58 (2001) 625–635.
[19] S.A. Wolfe, L. Nekludova, C.O. Pabo, DNA recognition by Cys2His2 zinc finger proteins, Annu. Rev. Biophys. Biomol. Struct. 29 (2000) 183–212.
[20] J.H. Laity, H.J. Dyson, P.E. Wright, Molecular basis for modulation of biological function by alternate splicing of the Wilms' tumor suppressor protein, Proc. Natl. Acad. Sci. U. S. A. 97 (2000) 11932–11935.
[21] G. Zhai, M. Iskandar, K. Barilla, P.J. Romaniuk, Characterization of RNA aptamer binding by the Wilms' tumor suppressor protein WT1, Biochemistry 40 (2001) 2032–2040.
[22] W.P. Yang, H. Wu, C.F. Barbas III, Surface plasmon resonance based kinetic studies of zinc finger–DNA interactions, J. Immunol. Methods 183 (1995) 175–182.
[23] E. Nurmemmedov, M. Thunnissen, Expression, purification, and characterization of the 4 zinc finger region of human tumor suppressor WT1, Protein Expr. Purif. 46 (2006) 379–389.
[24] X. Meng, M.H. Brodsky, S.A. Wolfe, A bacterial one-hybrid system for determining the DNA-binding specificity of transcription factors, Nat. Biotechnol. 23 (2005) 988–994.
[25] K. Bondeson, A. Frostell-Karlsson, L. Fagerstam, G. Magnusson, Lactose repressor–operator DNA interactions: kinetic analysis by a surface plasmon resonance biosensor, Anal. Biochem. 214 (1993) 245–251.
[26] F. Cornille, P. Emery, W. Schuler, C. Lenoir, B. Mach, et al., DNA binding properties of a chemically synthesized DNA binding domain of hRFX1, Nucleic Acids Res. 26 (1998) 2143–2149.
[27] S.M. Hamdan, B. Marintcheva, T. Cook, S.J. Lee, S. Tabor, et al., A unique loop in T7 DNA polymerase mediates the binding of helicase–primase, DNA binding protein, and processivity factor, Proc. Natl. Acad. Sci. U. S. A. 102 (2005) 5096–5101.
[28] B. Persson, K. Stenhag, P. Nilsson, A. Larsson, M. Uhlen, et al., Analysis of oligonucleotide probe affinities using surface plasmon resonance: a means for mutational scanning, Anal. Biochem. 246 (1997) 34–44.
[29] G. Witte, C. Urbanke, U. Curth, DNA polymerase III chi subunit ties single-stranded DNA binding protein to the bacterial replication machinery, Nucleic Acids Res. 31 (2003) 4434–4440.
[30] E.T. Young, N. Kacherovsky, C. Cheng, An accessory DNA binding motif in the zinc finger protein Adr1 assists stable binding to DNA and can be replaced by a third finger, Biochemistry 39 (2000) 567–574.
[31] T. Moss, DNA–protein interactions, principles and protocols, Methods in Molecular Biology 2nd ed., Humana Press, Totowa NJ, 2001.
[32] M. Oda, K. Furukawa, A. Sarai, H. Nakamura, Construction of an artificial tandem protein of the c-Myb DNA-binding domain and analysis of its DNA binding specificity, Biochem. Biophys. Res. Commun. 262 (1999) 94–97.
[33] S.C. Gill, P.H. von Hippel, Calculation of protein extinction coefficients from amino acid sequence data, Anal. Biochem. 182 (1989) 319–326.
[34] M.M. Bradford, A rapid and sensitive method for the quantitation of microgram quantities of protein utilizing the principle of protein-dye binding, Anal. Biochem. 72 (1976) 248–254.
[35] O.H. Lowry, N.J. Rosebrough, A.L. Farr, R.J. Randall, Protein measurement with the Folin phenol reagent, J. Biol. Chem. 193 (1951) 265–275.
[36] X. Meng, S.A. Wolfe, Identifying DNA sequences recognized by a transcription factor using a bacterial one-hybrid system, Nat Protoc 1 (2006) 30–45.
[37] T.L. Bailey, M. Boden, F.A. Buske, M. Frith, C.E. Grant, et al., MEME SUITE: tools for motif discovery and searching, Nucleic Acids Res. 37 (2009) W202–W208.
[38] G.E. Crooks, G. Hon, J.M. Chandonia, S.E. Brenner, WebLogo: a sequence logo generator, Genome Res. 14 (2004) 1188–1190.
[39] R. Karlsson, P.S. Katsamba, H. Nordin, E. Pol, D.G. Myszka, Analyzing a kinetic titration series using affinity biosensors, Anal. Biochem. 349 (2006) 136–147.
[40] R.W. Kriwacki, S.C. Schultz, T.A. Steitz, J.P. Caradonna, Sequence-specific recognition of DNA by zinc-finger peptides derived from the transcription factor Sp1, Proc. Natl. Acad. Sci. U. S. A. 89 (1992) 9759–9763.
[41] L.E. Schaufler, R.E. Klevit, Mechanism of DNA binding by the ADR1 zinc finger transcription factor as determined by SPR, J. Mol. Biol. 329 (2003) 931–939.
[42] R.R. Beerli, C.F. Barbas III, Engineering polydactyl zinc-finger transcription factors, Nat. Biotechnol. 20 (2002) 135–141.
[43] P. Blancafort, L. Magnenat, C.F. Barbas III, Scanning the human genome with combinatorial transcription factor libraries, Nat. Biotechnol. 21 (2003) 269–274.
[44] C.O. Pabo, E. Peisach, R.A. Grant, Design and selection of novel Cys2His2 zinc finger proteins, Annu. Rev. Biochem. 70 (2001) 313–340.
[45] K.R. Clemens, V. Wolf, S.J. McBryant, P. Zhang, X. Liao, et al., Molecular basis for specific recognition of both RNA and DNA by a zinc finger protein, Science 260 (1993) 530–533.
[46] D.R. Setzer, S.R. Menezes, S. Del Rio, V.S. Hung, G. Subramanyan, Functional interactions between the zinc fingers of Xenopus transcription factor IIIA during 5S rRNA binding, RNA 2 (1996) 1254–1269.
[47] O. Theunissen, F. Rudt, T. Pieler, Structural determinants in 5S RNA and TFIIIA for 7S RNP formation, Eur. J. Biochem. 258 (1998) 758–767.
[48] O. Theunissen, F. Rudt, U. Guddat, H. Mentzel, T. Pieler, RNA and DNA binding zinc fingers in Xenopus TFIIIA, Cell 71 (1992) 679–690.

[49] M.A. Searles, D. Lu, A. Klug, The role of the central zinc fingers of transcription factor IIIA in binding to 5S RNA, J. Mol. Biol. 301 (2000) 47–60.
[50] S. Del Rio, S.R. Menezes, D.R. Setzer, The function of individual zinc fingers in sequence-specific DNA recognition by transcription factor IIIA, J. Mol. Biol. 233 (1993) 567–579.
[51] T.B. Hamilton, J. Turner, K. Barilla, P.J. Romaniuk, Contribution of individual amino acids to the nucleic acid binding activities of the Xenopus zinc finger proteins TFIIIIA and p43, Biochemistry 40 (2001) 6093–6101.
[52] W.Q. Zang, N. Veldhoen, P.J. Romaniuk, Effects of zinc finger mutations on the nucleic acid binding activities of Xenopus transcription factor IIIA, Biochemistry 34 (1995) 15545–15552.
[53] H. Wang, R. Sun, G. Liu, M. Yao, J. Fei, et al., Characterization of the target DNA sequence for the DNA-binding domain of zinc finger protein 191, Acta Biochim. Biophys. Sin. (Shanghai) 40 (2008) 704–710.
[54] T.B. Hamilton, F. Borel, P.J. Romaniuk, Comparison of the DNA binding characteristics of the related zinc finger proteins WT1 and EGR1, Biochemistry 37 (1998) 2051–2058.
[55] J.H. Laity, J. Chung, H.J. Dyson, P.E. Wright, Alternative splicing of Wilms' tumor suppressor protein modulates DNA binding activity through isoform-specific DNA-induced conformational changes, Biochemistry 39 (2000) 5341–5348.
[56] A. Hammes, J.K. Guo, G. Lutsch, J.R. Leheste, D. Landrock, et al., Two splice variants of the Wilms' tumor 1 gene have distinct functions during sex determination and nephron formation, Cell 106 (2001) 319–329.
[57] P.A. Reynolds, G.A. Smolen, R.E. Palmer, D. Sgroi, V. Yajnik, et al., Identification of a DNA-binding site and transcriptional target for the EWS–WT1(+KTS) oncoprotein, Genes Dev. 17 (2003) 2094–2107.
[58] H. Li, G.A. Smolen, L.F. Beers, L. Xia, W. Gerald, et al., Adenosine transporter ENT4 is a direct target of EWS/WT1 translocation product and is highly expressed in desmoplastic small round cell tumor, PLoS ONE 3 (2008) e2353.
[59] R. Stoll, B.M. Lee, E.W. Debler, J.H. Laity, I.A. Wilson, et al., Structure of the Wilms tumor suppressor protein zinc finger domain bound to DNA, J. Mol. Biol. 372 (2007) 1227–1245.
[60] N. Bardeesy, J. Pelletier, Overlapping RNA and DNA binding domains of the wt1 tumor suppressor gene product, Nucleic Acids Res. 26 (1998) 1784–1792.
[61] W.L. Gerald, D.A. Haber, The EWS–WT1 gene fusion in desmoplastic small round cell tumor, Semin. Cancer Biol. 15 (2005) 197–205.
[62] L. Fairall, S.D. Harrison, A.A. Travers, D. Rhodes, Sequence-specific DNA binding by a two zinc-finger peptide from the Drosophila melanogaster Tramtrack protein, J. Mol. Biol. 226 (1992) 349–366.
[63] K. Sakaguchi, E. Appella, J.G. Omichinski, G.M. Clore, A.M. Gronenborn, Specific DNA binding to a major histocompatibility complex enhancer sequence by a synthetic 57-residue double zinc finger peptide from a human enhancer binding protein, J. Biol. Chem. 266 (1991) 7306–7311.